Structural Engineering and Mechanics, Vol. 9, No. 1 (2000) 99-110
DOI: http://dx.doi.org/10.12989/sem.2000.9.1.099

Geometrically nonlinear analysis of laminated composites by an improved degenerated shell element

Seung-Woon Yoo†

Department of Civil Engineering, Kwandong University, Kangwon 215-800, Korea

Chang-Koon Choi‡

Department of Civil Engineering, KAIST, Taejon 305-701, Korea

Abstract. The objective of this paper is to extend the use of the improved degenerated shell element to the linear and the large displacement analysis of plates and shells with laminated composites. In the formulation of the element stiffness, the combined use of three different techniques was made. This element is free of serious shear/membrane locking problems and undesirable compatible/commutable spurious kinematic deformation modes. The total Lagrangian approach has been utilized for the definition of the deformation and the solution to the nonlinear equilibrium equations is obtained by the Newton-Raphson method. The applicability and accuracy of this improved degenerated shell element in the analysis of laminated composite plates and shells are demonstrated by solving several numerical examples.

Key words: geometrically nonlinear; laminated composite; nonconforming mode; shell element.

1. Introduction

The analysis of plate and shell structures has been one of the major research interests for many structural engineers because of the technological importance of such structures. Quite often these structures are constructed of laminated composites due to the high specific stiffness and strength of composite structures. However, the analysis of such structures requires computational techniques such as the finite element method because the large displacements and rotations constitute a major part of the overall motion (Madenci and Barut 1994).

A number of different element types have been proposed for the finite element analysis of shell structures in the past. As for the description of the geometry and kinematics of deformation, the degenerated shell concept (Ahmad *et al.* 1970), among others, may be one of the most convenient. This element adopts the basic assumptions of the shell theory which allow the transverse shear deformation and the isoparametric representation in the finite element approximation. As such it can be applied to the finite element modeling of arbitrary shell geometries, and geometrically and materially nonlinear shell structures without resorting to a particular shell theory (Ramm and Matzenmiller 1986).

† Associate Professor
‡ Institute Chair Professor

Although the degenerated shell element seemed to be promising when it was first introduced, the performance of such elements was found to be rapidly deteriorating as the shell thickness becomes thin. This problem, known as the shear or membrane locking phenomenon, may lead to unreliable results in some cases. These phenomena are associated with the over-constraining of the zero transverse shear strain and the zero membrane strain conditions for thin shells. Recently an improved degenerated shell element that is free of serious shear/membrane locking and commutable spurious kinematic mode has been proposed for analysis of isotropic shells undergoing small and large deflection (Choi and Yoo 1991a, b). In the formulation of these shell elements, several schemes are simultaneously used in a complementary way. These schemes include a modified version of the assumed transverse shear strain method to overcome the shear locking problems, the reduced integration of the in-plane strains to alleviate the membrane locking problems, and the addition of the nonconforming displacement modes to improve the general performance of the element.

The main objective of this paper is to extend the use of the improved degenerated shell element to the small and large displacement analyses of plates and shells with laminated composites. The total Lagrangian approach has been utilized for the definition of the deformation, and the solution to the nonlinear equilibrium equations is obtained by the Newton-Raphson method.

2. Nonlinear finite element formulation

2.1. Geometry and kinematic equations for shells

In this section, the underlying basic ideas in formulation of the degenerated curved shell element are described briefly. The geometry of a shell can be represented by the coordinates and normal vectors of its middle surface as shown in Fig. 1.

In degenerated isoparametric formulation, the displacement field can be expressed in terms of the nodal unknowns defined at the mid-surface of the element as

$$\begin{bmatrix} u \\ v \\ w \end{bmatrix} = \sum_{k=1}^{n} N_k(\xi, \eta)\,\zeta \begin{bmatrix} u_k \\ v_k \\ w_k \end{bmatrix}_{mid} + \sum_{k=1}^{n} N_k(\xi, \eta)\,\zeta\,\boldsymbol{b}_k \tag{1}$$

where

$$\boldsymbol{b}_k = \frac{h_k}{2}(\bar{\boldsymbol{v}}'_3 - \bar{\boldsymbol{v}}_3)_k \tag{2}$$

In Eq. (1), n is the number of nodes per element; $N_k(\xi, \eta)$ are the element shape functions corresponding to the surface ζ; h_k is the shell thickness at node k; and ξ, η and ζ are the curvilinear coordinates of the point under consideration. The vector $\boldsymbol{v}_{3k}$ is constructed from the nodal coordinates of the top and bottom surface at node k; thus, $\boldsymbol{v}_{3k} = \boldsymbol{x}_k^{top} - \boldsymbol{x}_k^{bot}$, where $\boldsymbol{x}_k = [x_k\ y_k\ z_k]^T$. The unit vectors in the directions of $\boldsymbol{v}_{3k}$ are represented by $\bar{\boldsymbol{v}}_{3k}$.

In Eq. (2) $\bar{\boldsymbol{v}}'_3$ denotes $\bar{\boldsymbol{v}}_3$ in the deformed configuration. If the deformation of $\bar{\boldsymbol{v}}_3$ to $\bar{\boldsymbol{v}}'_3$ is described as rotation α around $\bar{\boldsymbol{v}}_2$ and β around $\bar{\boldsymbol{v}}_1$, $\boldsymbol{b}_k$ can be rewritten as (Surana 1983)

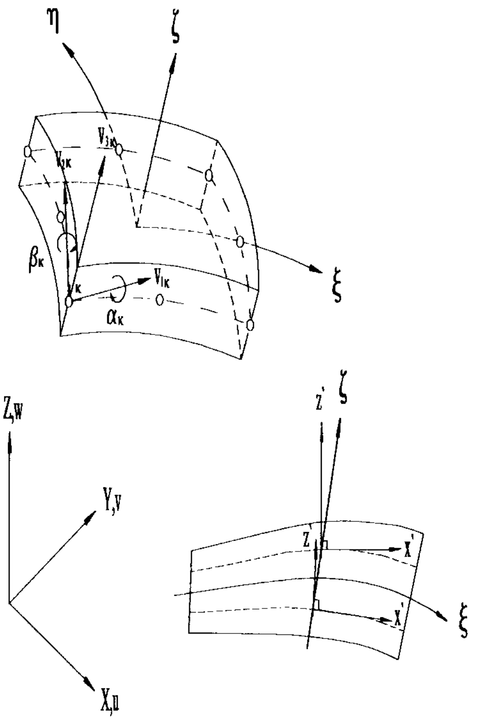

Fig. 1 Coordinate systems in degenerated shell element

$$\boldsymbol{b}_k=\frac{h_k}{2}\left[\sin\alpha\cos\beta\bar{\boldsymbol{v}}'_1-\sin\beta\bar{\boldsymbol{v}}_2+(\sin\alpha\cos\beta-1)\bar{\boldsymbol{v}}_3\right]_k \tag{3}$$

The Green-Lagrangian strain vector can be determined from the displacement field using the strain-displacement relations as

$$\boldsymbol{\varepsilon}=\boldsymbol{\varepsilon}^o+\boldsymbol{\varepsilon}^L \tag{4}$$

where $\boldsymbol{\varepsilon}^o$ and $\boldsymbol{\varepsilon}^L$ are, respectively, the linear and nonlinear parts of the Green-Lagrangian strain vector, and defined as

$$\boldsymbol{\varepsilon}^o=\begin{bmatrix} u'_{,x'} \\ v'_{,y'} \\ u'_{,y'}+v'_{,x} \\ u'_{,z'}+w'_{,x'} \\ v'_{,z'}+w'_{,y'} \end{bmatrix} \tag{5}$$

$$\varepsilon^L=\begin{bmatrix} \frac{1}{2}[(u'_{,x'})^2+(v'_{,x'})^2+(w'_{,x'})^2] \\ \frac{1}{2}[(u'_{,y'})^2+(v'_{,y'})^2+(w'_{,y'})^2] \\ u'_{,x'}u'_{,y'}+v'_{,x'}v'_{,y'}+w'_{,x'}w'_{,y'} \\ u'_{,x'}u'_{,z'}+v'_{,x'}v'_{,z'}+w'_{,x'}w'_{,z'} \\ u'_{,y'}u'_{,z'}+v'_{,y'}v'_{,z'}+w'_{,y'}w'_{,z'} \end{bmatrix} \tag{6}$$

Let

$$\boldsymbol{E}=[\boldsymbol{E}_{x'},\ \boldsymbol{E}_{y'},\ \boldsymbol{E}_{z'}]^T \tag{7}$$

where

$$\boldsymbol{E}_{x'}=[u'_{,x'},\ v'_{,x'},\ w'_{,x'}]^T \quad \boldsymbol{E}_{y'}=[u'_{,y'},\ v'_{,y'},\ w'_{,y'}]^T \quad \boldsymbol{E}_{z'}=[u'_{,z'},\ v'_{,z'},\ w'_{,z'}]^T \tag{8}$$

Then, ε^o and ε^L can be represented in matrix form as

$$\varepsilon^o=\begin{bmatrix} 1\,0\,0 & 0\,0\,0 & 0\,0\,0 \\ 0\,0\,0 & 0\,1\,0 & 0\,0\,0 \\ 0\,1\,0 & 1\,0\,0 & 0\,0\,0 \\ 0\,0\,1 & 0\,0\,0 & 1\,0\,0 \\ 0\,0\,0 & 0\,0\,1 & 0\,1\,0 \end{bmatrix}\boldsymbol{E}=\boldsymbol{HE} \tag{9}$$

where $\boldsymbol{H}$ is a constant matrix and

$$\varepsilon^L=\frac{1}{2}\begin{bmatrix} \boldsymbol{E}_{x'}^T & 0 & 0 \\ 0 & \boldsymbol{E}_{y'}^T & 0 \\ \boldsymbol{E}_{y'}^T & \boldsymbol{E}_{x'}^T & 0 \\ \boldsymbol{E}_{z'}^T & 0 & \boldsymbol{E}_{x'}^T \\ 0 & \boldsymbol{E}_{z'}^T & \boldsymbol{E}_{y'}^T \end{bmatrix}\boldsymbol{E}=\frac{1}{2}\boldsymbol{AE} \tag{10}$$

in which $\boldsymbol{A}$ is dependent on the nodal degrees of freedom vector $\boldsymbol{u}$.

Using above Eq. (4), the variations of linear and nonlinear strains can be written as

$$d\varepsilon = d\varepsilon^o + d\varepsilon^L = \boldsymbol{H}d\boldsymbol{E} + \boldsymbol{A}d\boldsymbol{E} \tag{11}$$

where

$$d\boldsymbol{E} = \boldsymbol{G}d\boldsymbol{u} \tag{12}$$

Therefore

$$d\varepsilon = \boldsymbol{B}d\boldsymbol{u} \tag{13}$$

where

$$\boldsymbol{B} = \boldsymbol{B}^o + \boldsymbol{B}^L = [\boldsymbol{H} + \boldsymbol{A}]\,\boldsymbol{G} \tag{14}$$

2.2. Discretized equilibrium equation

The discretized equilibrium equations for the structure are derived via the virtual work expression which, in its finite element total Lagrangian form, can be written as

$$\boldsymbol{\Psi}=\boldsymbol{R}-\int_V \boldsymbol{B}^T\sigma\, dV=\boldsymbol{R}-\boldsymbol{P} \tag{15}$$

The residual $\boldsymbol{\Psi}$ can be visualized as the nodal forces required to bring the assumed displacement pattern into nodal equilibrium. $\boldsymbol{R}$ is the equivalent nodal force vector due to exterior loads. Since Eq. (15) cannot be solved directly for deflection $\boldsymbol{u}$, we derive an incremental equation of equilibrium from Eq. (15) and set up an iterative procedure for its solution.

Taking variation of Eq. (15)

$$\begin{aligned} d\boldsymbol{\Psi}&=d\boldsymbol{R}-\int_V \boldsymbol{B}^T d\sigma\, dV-\int_V d\boldsymbol{B}^T\sigma\, dV \\ &=d\boldsymbol{R}-\int_V \boldsymbol{B}^T d\sigma\, dV-\int_V \boldsymbol{G}^T d\boldsymbol{A}^T\sigma\, dV-\int_V d\boldsymbol{G}^T[\boldsymbol{H}+\boldsymbol{A}]^T\sigma\, dV \end{aligned} \tag{16}$$

where

$$\int_V \boldsymbol{B}^T d\sigma\, dV=\int_V \boldsymbol{B}^T\boldsymbol{D}\boldsymbol{B}\, dV d\boldsymbol{u}=\boldsymbol{K}_0 d\boldsymbol{u} \tag{17a}$$

$$\int_V \boldsymbol{G}^T d\boldsymbol{A}^T\sigma\, dV=\int_V \boldsymbol{G}^T\boldsymbol{S}\boldsymbol{G}\, dV d\boldsymbol{u}=\boldsymbol{K}_{\sigma 1} d\boldsymbol{u} \tag{17b}$$

$$\int_V d\boldsymbol{G}^T[\boldsymbol{H}+\boldsymbol{A}]^T\sigma\, dV=\boldsymbol{K}_{\sigma 2} d\boldsymbol{u} \tag{17c}$$

where

$$\boldsymbol{S}=\begin{bmatrix} \sigma_{x'}\boldsymbol{I} & \tau_{x'y'}\boldsymbol{I} & \tau_{x'z'}\boldsymbol{I} \\ \tau_{x'y'}\boldsymbol{I} & \sigma_{x'}\boldsymbol{I} & \tau_{y'z'}\boldsymbol{I} \\ \tau_{x'z'}\boldsymbol{I} & \tau_{y'z'}\boldsymbol{I} & 0 \end{bmatrix}, \quad \boldsymbol{I}=\begin{bmatrix} 1 & 0 & 0 \\ 0 & 1 & 0 \\ 0 & 0 & 1 \end{bmatrix} \tag{18}$$

Thus the incremental form of the equilibrium equation given by Eq. (15) can be written as

$$d\boldsymbol{\Psi}=d\boldsymbol{R}-[\boldsymbol{K}_0+\boldsymbol{K}_{\sigma 1}+\boldsymbol{K}_{\sigma 2}]d\boldsymbol{u}=d\boldsymbol{R}-\boldsymbol{K}_T d\boldsymbol{u} \tag{19}$$

where $\boldsymbol{K}_T$ is the symmetric tangent stiffness matrix.

2.3. Material modeling

The shell structures under consideration may have laminated material construction, whereby each layer can be an orthotropic material with a given orientation as shown in Fig. 2. Each lamina or ply of the laminate may have different material properties and different ply angles. The stress-strain relationship of the i-th layer with respect to the local coordinate system is expressed as

$$d\sigma=\boldsymbol{D}^*\, d\varepsilon \tag{20}$$

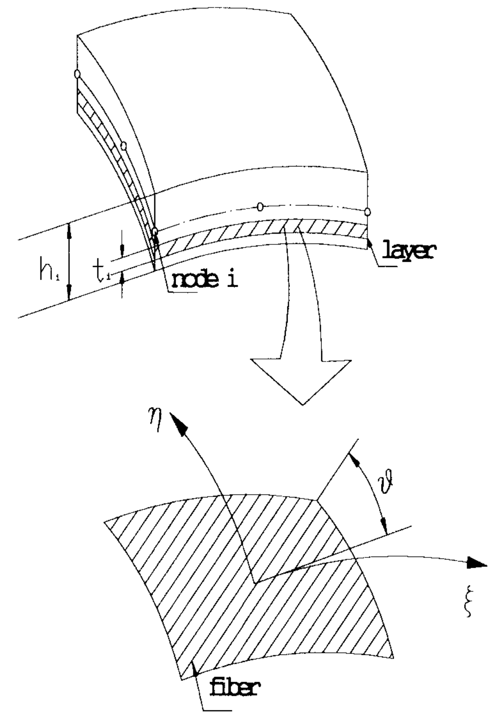

Fig. 2 Geometry of laminated shell element

where D^* is elastic constant matrix. Since the shell is assumed to be relatively thin, the stress component normal to the middle surface can be ignored (Panda and Natarajan 1981, Kim and Lee 1992). It is obvious that the elasticity matrix is dependent on fiber orientation and in general is different for each lamina.

In this paper, the term "composite" is used to denote a material system made up of one or more than one material in the form of layers stacked on top of each other. Each material may possess either isotropic or orhtotropic properties, which are assumed to be uniform throughout the continuum of the material. The bonding of layers is assumed to be perfect and no slippage is considered.

The objective of this paper is to extend the use of an improved degenerated shell element presented by author (Choi and Yoo 1991a) to the small and large deflection analysis of laminated composites. In this analysis, a simple numerical integration of thickness is adopted for the treatment of layer stacking effect. The integration of the stiffness matrix is performed for each layer to capture its material property. This is achieved by modifying the variable ζ to ζ_i in any i-th layer such that ζ_i varies from -1 to 1 in that layer. The integration over the shell thickness direction is achieved by summing up the contribution of each layer (Panda and Natarajan 1981), such that

$$K_T = \sum_{i=1}^{nl} \iiint_{-1}^{+1} f(\xi, \eta, \zeta) |J| \frac{t_i}{h} d\xi\, d\eta\, d\zeta_i \tag{21}$$

and nl is the total number of layers in the shell numbered from the bottom $\zeta = -1$; $|J|$ is Jacobian determinant; h is total thickness of shell; and t_i is i-th layer thickness.

3. Improved degenerated shell element formulation

The reduction in the order of integration in computing the stiffness matrix of an isoparametric element may eliminate some of the extraneous shear and membrane strains imposed by the displacement constraints and results in obtaining some improvement in the element behavior (Zienkiewicz *et al.* 1971). It is observed, however, that some of the reduced integrated elements have deficiencies. An 8-node reduced integrated element may produce the shear locking phenomena in plate bending problems below a certain thickness-length ratio, and the 4-node and 9-node elements of the Lagrangian family display the undesirable compatible/commutable spurious zero (or low) energy modes (Parisch 1979).

Another way to improve the basic accuracy of the isoparametric element is by substituting assumed transverse shear strain fields (Dvorkin and Bathe 1984). In this paper, the modification of the technique for a quadratic element has been suggested. The basic form of displacement field is modified by the addition of nonconforming displacement mode bar $\overline{N}_5$ to translational d.o.f. in the 8-node serendipity element whereas the previous studies were based on either 8-node, or 9-node Lagrangian formulation (Huang and Hinton 1986). Therefore, the substitutional transverse shear strains should be taken as polynomials of at least the same degrees (Choi and Yoo 1991a) as those of a 9-node Lagrangian element.

One of the main causes of inaccuracies in the solutions obtained by the isoparametric elements is their inability to represent certain simple stress gradients. The technique improves the basic accuracy of the isoparametric element by eliminating the excessive strain through the addition of

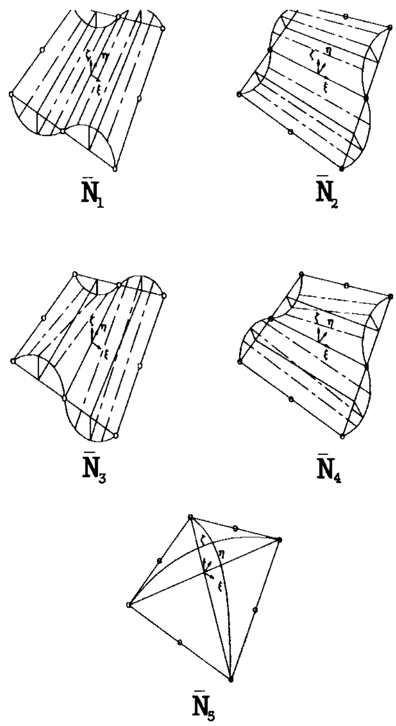

Fig. 3 Nonconforming displacement modes

nonconforming displacement modes (Choi and Schnobrich 1975, Choi *et al.* 1998).

The possible nonconforming displacement modes to be added to the quadratic serendipity element are suggested by Choi and Schnobrich (1975) (see Fig. 3).

$$\bar{N}_1=\xi(1-\xi^2),\quad \bar{N}_2=\eta(1-\eta^2)$$
$$\bar{N}_3=\xi\eta(1-\xi^2),\quad \bar{N}_4=\xi\eta(1-\eta^2),\quad \bar{N}_5=(1-\xi^2)(1-\eta^2) \tag{22}$$

The additional modes are so selected that they have zero values at each node and eliminate the undesirable constraints present in the original isoparametric shapes.

The general form of the displacement field in the degenerated shell element of a previous work (Choi and Schnobrich 1975) was formed by adding nonconforming modes in Eq. (22) selectively to the original displacement of the element. With five nonconforming modes added selectively to mid-surface displacement components (u, v, w), the displacement field can be compactly expressed as

$$\boldsymbol{U}=\sum_{i=1}^{8} N_i\boldsymbol{u}_i+\sum_{i=1}^{5} \bar{N}_j\bar{\boldsymbol{u}}_j \tag{23}$$

Note that the additional degrees of freedom $\bar{\boldsymbol{u}}_j$ are interpreted as the amplitudes of the added displacement modes rather than physical displacements at nodes. The resulting stiffness matrix has been enlarged over the original shell element because of the unknowns corresponding to the additional modes. The augmented stiffness matrix can be condensed back to the same order as the original element stiffness matrix.

The above concepts were extended to develop a new shell element (Choi and Yoo 1991a, Choi *et al.* 1998) that is further improved by the combined use of above techniques in complementary way, i.e., overcoming the shear locking problem by substituting the shear strain fields, avoiding the membrane locking behavior by reduced integration, and improving the element performance by adding nonconforming displacement modes. In this paper, the application of this shell element was extended to the small and large displacement analysis of shells constructed with laminated composites.

Separating the overall element stiffness into the in-plane stiffness (i.e., the combined membrane and bending effects) and the transverse shear stiffness, the shear strains are interpolated from the values at certain sampling points to eliminate the shear locking problems and the in-plane stiffness is computed with reduced integration in order to avoid the membrane locking problems. All five nonconforming displacement modes are then added to the element stiffness components to improve the overall performance of the element. In the evaluation of shear stiffness of an element, the 2×3/3×2 integration is used while the in-plane stiffness is computed with the reduced integration order (2×2 integration).

The relationship between the displacement derivatives and displacements is expressed in the following form.

$$d\boldsymbol{E}=\boldsymbol{G}d\boldsymbol{u}_t=\sum_{i=1}^{8}\begin{bmatrix}\boldsymbol{G}_f\\ \tilde{\boldsymbol{G}}_s\end{bmatrix}d\boldsymbol{u}+\sum_{j=1}^{5}\begin{bmatrix}\bar{\boldsymbol{G}}_f\\ \bar{\boldsymbol{G}}_s\end{bmatrix}d\bar{\boldsymbol{u}} \tag{24}$$

where the vectors $d\boldsymbol{u}$ and $d\bar{\boldsymbol{u}}$ are defined as $d\boldsymbol{u}$ = $[du\ dv\ dw\ d\alpha\ d\beta]^T$, $d\bar{\boldsymbol{u}}=[d\bar{u}\ d\bar{v}\ d\bar{w}\ 0\ 0]^T$. In Eq. (24), the matrix $\boldsymbol{G}_f$ contains the incremental in-plane displacement derivatives, $\tilde{\boldsymbol{G}}_s$ the incremental substituted shear displacement derivatives, $\bar{\boldsymbol{G}}_f$, $\bar{\boldsymbol{G}}_s$ the incremental displacement derivatives related to nonconforming displacement modes, and $\bar{\boldsymbol{u}}$ is additional degrees of freedom corresponding to the nonconforming displacement modes.

4. Numerical Examples

The results obtained for several sample problems are compared with other elements such as QSR (Zienkiewicz *et al.* 1971) which is an 8-node isoparametric element with fully reduced integration. The resulting non-linear equilibrium equations are solved by the Newton-Raphson method. The iteration was terminated when the Euclidian norms of incremental degrees of freedom vectors became less than 10^{-3} times the Euclidian norms of total degrees of freedom vectors.

4.1. Cross-ply laminated plate under uniform loading

In the analysis of laminated composite plates, cross-ply laminates have been given considerable attention. The cross-ply lay-up is a special case of the general angle-ply layer arrangement. If each layer of a laminate is orthotropic, the laminate exhibits orthotropic property as an whole.

A nine layers cross-ply symmetrically laminated square plate is considered here. The detail lay-up is (0/90/0/90/0/90/0/90/0), where the numbers indicate the fibre orientation for each layer and they are in degrees. The thicknesses of 0^o and 90^o layers are the same. The simply supported and clamped square plate subjected to a uniformly distributed pressure q is analyzed to test the performance of the present improved degenerated shell element for laminated composite analysis. The following geometric and material parameters are used: $b = 10$ in, $h = 0.02$ in, $E_1 = 3.0\times10^7$ psi, $E_2 = 0.75\times10^6$ psi, $G_{12} = 0.45\times10^6$ psi, $G_{13} = G_{23} = 0.375\times10^6$ psi, and $\nu = 0.25$. Owing to symmetrical conditions that the problem has, one quarter of the laminated plate is modeled. Results are compared with a solution adopted by Wang (1995). A rapid convergence of the solutions by the present element is apparent for this problem as shown in Fig. 4.

4.2. Angle-ply ($\pm\theta$) laminated plate under uniform loading

The next example problem considered is a 2 layer laminated plate lay up ($\pm\theta$). The simply supported square plate is subjected to a uniformly distributed pressure q and analyzed to test the performance of the present improved degenerated shell element for laminated composite analysis. Entire plate is modeled by N×N mesh because of the existence of the fiber-orientation-induced

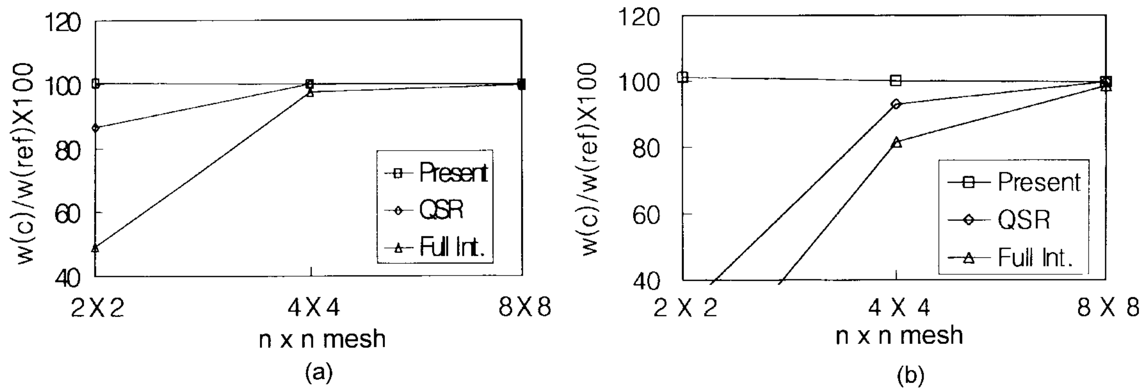

Fig. 4 (a) Convergence characteristics for central deflection of layered plate (simply supported), (b) Convergence characteristics for central deflection of layered plate (clamped)

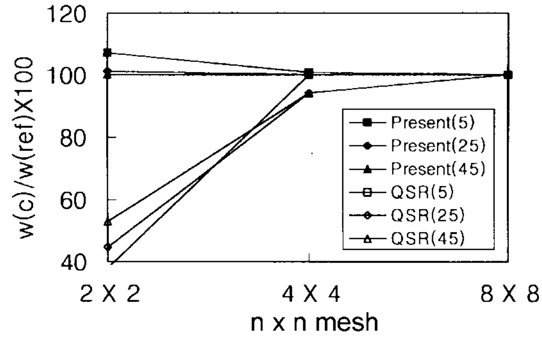

Fig. 5 Convergence characteristics for central deflection of layered plate ($\pm\theta$)

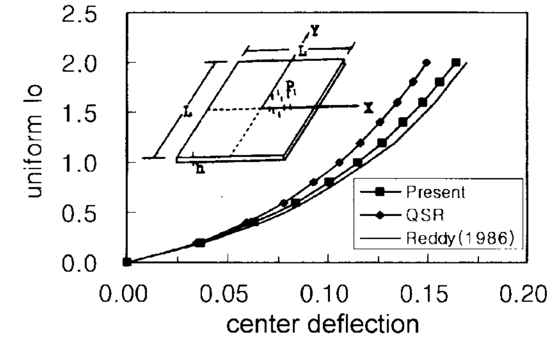

Fig. 6 Load-deflection for 4 layer (0/90/0/90) clamped plate in large deformation

bending and stretching coupling which eliminates the usual x-y plane symmetries. The following geometric and material parameters are used; $b = 10$ in, $h = 0.02$ in, $E_1 = 40\times10^6$ psi, $E_2 = 1.0\times10^6$ psi, $G_{12} = G_{23} = 0.5\times10^6$ psi, $\nu = 0.25$. The convergence was studied by modeling the whole square plate with the varying angle of θ. Results will be compared with a series solution adopted by Spilker (1982). A rapid convergence of the solutions by the present element is apparent for this problem as shown in Fig. 5.

4.3. 4 layer (0/90/0/90) clamped plate for large deformation

The problem under consideration in this example is the large deformation of a 4 layer (0/90/0/90) clamped plate under uniformly distributed load. The following geometric and material parameters are used: $L = 12$ in, $h = 0.096$ in, $E_1 = 1.828\times10^6$ psi, $E_2 = 1.832\times10^6$ psi, $G_{12} = G_{13} = G_{23} = 0.3125\times10^6$ psi, and $\nu = 0.23949$. Because of the symmetry of the structure, only a quarter of the plate is modeled with 44 mesh. Fig. 6 shows the vertical deflections at the center of the plate under increasing uniformly distributed load and the comparison with those obtained by Reddy (1986).

4.4. 3 layer (0/90/0) hinged cylindrical shell for large deformation

The last example problem is a 3 layer cross-ply (0/90/0) hinged cylindrical shell under point load

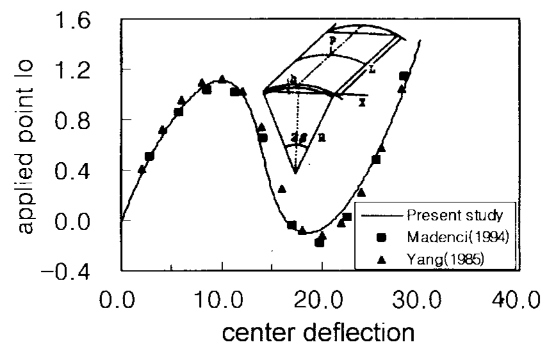

Fig. 7 Load-deflection for 3 layer (0/90/0) hinged cylindrical shell in large deformation

for large deformation analysis. The boundary conditions are such that the curved edges are free while the straight edges are hinged. The cylindrical shell geometry is shown in Fig. 7. The length of cylindrical shell is 508 mm and the radius of curvature is 2540 mm. The total angle specifying the width is 0.2 radian and the thickness of shell is 12.6 mm. Each lamina has the properties $E_1 = 3.3$ GPa, $E_2 = 1.1$ GPa, $G_{12} = 0.66$ GPa, $G_{23} = 0.44$ GPa and $\nu = 0.25$. A quarter of the shell is modeled with a 4×4 mesh because of the symmetry of the structure. In Fig. 7, the numerical results obtained for the deflection at the center of shell are compared with those obtained by Madenci (1994) and Yang (1986). Good agreements between the results are observed for this problem.

5. Conclusions

This paper is concerned with the linear and geometrically nonlinear analysis of laminated composite shell structures using an improved degenerated shell element. The present shell elements are based on the degenerated shell element which has been improved by the combined use of three different techniques in complementary way. These schemes include a modified version of the assumed transverse shear strain method to overcome the shear locking problems, the reduced integration of the in-plane strains to alleviate the membrane locking problems, and the addition of the nonconforming displacement modes to improve the general performance of the element.

The results of numerical examples demonstrate the applicability of the present approach in modeling the linear and large deformation behavior of laminated composite plates and shells. The element derived for nonlinear analysis of laminated composite shells is based on a total Lagrangian formulations for arbitrarily large displacements and rotations. Numerical examples show that the present approach is capable of modeling composite thin plates and shells of arbitrary geometry and give good results for laminates.

Acknowledgements

This work was supported by grant No. 971-1203-013-2 from the Basic Research program of the KOSEF.

References

Ahmad, S., Irons, B.M. and Zienkiewicz, O.C. (1970), "Analysis of thick and thin shell structures by curved elements", *Int. J. Numer. Methods Eng.*, **2**, 491-451.

Choi, C.K. and Schnobrich, W.C. (1975), "Use of nonconforming modes in finite element analysis of shells", *J. Eng. Mech. Div., ASCE*, **101**, 447-464.

Choi, C.K. and Yoo, S.W. (1991a), "Combined use of multiple improvement techniques in degenerated shell element", *Computers and Structures*, **39**, 557-569.

Choi, C.K. and Yoo, S.W. (1991b), "Geometrically nonlinear behavior of an improved degenerated shell element", *Computers and Structures*, **40**, 785-794.

Choi, C.K. *et al.* (1998), "Two-dimensional nonconforming finite elements: A state-of-the-art", *Structural Engineering and Mechanics*, **6**(1), 41-61.

Dvorkin, E.N. and Bathe, K.J. (1984), "A continuum mechanics based four-node shell element for general

nonlinear analysis", *Engineering Computation*, **1**, 77-88.
Ganapathi, M. and Touratier, M. (1996), "A C^0 eight-node menbrane-shear-bending element for geometrically non-linear (static and dynamic) analysis of laminates", *Int. J. Numer. Methods Eng.*, **39**, 3453-3474.
Huang, H.C. and Hinton, E. (1986), "A new nine node degenerated shell element with enhanced membrane and shear interpolation", *Int. J. Numer. Methods Eng.*, **22**, 73-92.
Hughes, T.J.R., Cohen, M. and Haron, M. (1978), "Reduced and selective integration techniques in the finite element analysis of plates", *Nuclear Eng. Desgn.*, **46**, 203-22.
Kim, J.H. and Lee, S.W. (1992), "A finite element formulation with stabilization matrix for geometrically non-linear shells", *Int. J. Numer. Methods Eng.*, **33**, 1703-1720.
Kosmatka, J.B. (1994), "An accurate shear-deformable six-node triangular plate element for laminated composite structures", *Int. J. Numer. Methods Eng.*, **37**, 431-455.
Kumar, W.P.P. and Palaninathan, R. (1997), "Finite element analysis of laminated shells with exact through-thickness integration", *Computers and Structures*, **63**, 173-184.
Madenci, E. and Barut, A. (1994), "A free-formulation-based flat shell element for non-linear analysis of thin composite structures", *Int. J. Numer. Methods Eng.*, **37**, 3825-3842.
Panda, S. and Natarajan, R. (1981), "Analysis of laminated composite shell structures by finite element method", *Computers and Structures*, **14**, 225-230.
Parisch, H. (1979), "A critical survey of the 9-node degenerated shell element with special emphasis on thin shell application and reduced integration", *Comp. Meth. App. Mech. Eng.*, **20**, 323-350.
Ramm, E. and Matzenmiller, A. (1986), "Large deformation shell analyses based on the degenerated concept", *Finite Element Methods for Plate and Shell Structures* (Edited by T.J.R. Hughes and E. Hinton), Pineridge Press.
Reddy, J.N. (1986), "On mixed finite element formulations of a higher-order theory of composite laminates", *Finite Element Methods for Plate and Shell Structures*, (Edited by T.J.R. Hughes and E. Hinton), Pineridge Press.
Reddy, J.N. and Chandrashekhara, K. (1983), "Nonlinear analysis of laminated shells including transverse shell strains", *AIAA J.*, **23**, 440-441.
Saigal, S., Kapania, R.K. and Yang, T.Y. (1986), "Geometrically nonlinear finite element analysis of imperfect laminated shells", *J. Composite Materials*, **20**, 197-214.
Spilker, R.L. (1982), "Hybrid-stress eight-node elements for thin and thick multilayer laminated plates", *Int. J. Numer. Methods Eng.*, **18**, 801-826.
Surana, K.S. (1983), "Geometrically nonlinear formulation for the curved shell elements", *Int. J. Numer. Methods Eng.*, **19**, 581-615.
Wang, B. (1995), "Finite element analysis of geometrically nonlinear laminated composite shell structures", PhD dissertation, University of Western Ontario, Ontario, Canada.
Yeom, C.H. and Lee, S.W. (1989), "An assumed strain finite element model for large deflection composite shells", *Int. J. Numer. Methods Eng.*, **28**, 1749-1768.
Zienkiewicz, O.C., Taylor, R.L. and Too, J.M. (1971), "Reduced integration techniques in general analysis of plates and shells", *Int. J. Numer. Methods Eng.*, **3**, 275-290.